

Research Paper

Modeling the Propagation of Ultrasonic Guided Waves in a Composite Plate by a Spectral Approximation Method

Ismaine ZITOUNI*, Hassan RHIMINI, Abdelkerim CHOUAF

*Laboratory of Mechanics, Engineering and Innovation
National High School of Electricity and Mechanics, Hassan II University
Casablanca, Morocco*

*Corresponding Author e-mail: ismaïne.zitouni.doc20@ensem.ac.ma

Graphite-epoxy composites have been able to meet the multiple requirements of the space industry. However, the radiation from the spatial environment and non-perfect adhesion between the fibers and the matrix can lead to the appearance of imperfections. To handle this, we use non-destructive testing by ultrasonic guided waves known for its high accuracy in detecting defects. In this article, we study the propagation of ultrasonic guided waves in a graphite-epoxy composite plate by the spectral method. First, the mathematical formalism is explained for modeling guided waves in the composite material. Next, we plot the dispersion curves of the composite plate in different orientations of the fibers with a MATLAB program and the results are compared with those of the DISPERSE software. These give us information on the modes that propagate in the structure. We elaborate and explain a technique based on displacement symmetry to distinguish between the different modes. A discussion based on time-saving and accuracy is established to show the advantages of the method.

The second part of our paper consists in giving a physical meaning to the spectral displacements normalized in amplitude. We propose to normalize the spectral eigenvectors by the acoustic power. We plot the displacement and stress profiles of the guided modes and we compare our results to the analytical ones. Perfect correspondence is found, indicating the accuracy of the approach developed. In addition, a study of the vibrational state in the composite plate is established for Lamb and horizontal shear modes at a specific frequency.

Keywords: guided waves; spectral method; dispersion curves; graphite-epoxy composite; acoustic power; normalized displacement.

1. INTRODUCTION

Composite materials are widely used in the aeronautical, automotive and railway industries due to their lightness, performance, resistance to the loads and environmental conditions they endure. However, the inhomogeneity between the fibers and the matrix leads to the appearance of defects that can lead to functional failures [1, 2]. Therefore, adequate control of their quality is essential to ensure their integrity. Ultrasonic guided waves (UGW) have a great poten-

tial for non-destructive testing of composite structures due to their ability to propagate over a long distance without significant attenuation and to control the entire structure [3–5]. The most important steps for non-destructive testing by UGW are the knowledge of the dispersion curves and the shape of the mode. The dispersion curves present the frequency-wave number couple susceptible to propagate in the plate and detect the defects. The shape of the mode is crucial during the interaction of the wave with the defect. Several research works have focused on plotting the dispersion curves by different methods. We find methods based on the application of roots finding algorithms in the characteristic equations for different types of monolayer waveguides, and we cite the methods of bisection and Newton-Raphson [6, 7] or with the application of matrix method for multilayered system (stiffness matrix method (SMM), transfer matrix method (TMM), global matrix method (GMM) [8]. Others use numerical methods such as the orthogonal polynomial approach [9–11], where based on polynomial approximations, where viscoelastic cylindrical structures and the initially stressed plate are studied. We also cite the semi-analytical finite element method [12, 13] that has shown its great advantage in characterizing the dispersion of single and multilayer composite structures.

We also find the spectral method developed by ADAMOU and CRASTER [14] for the determination of the dispersion of UGW. This method has attracted the interest of several authors [15, 16]. It is based on the transformation of the partial differential equations of the problem into an algebraic system by approximating the solution with Chebyshev polynomials. The partial derivatives are then replaced by differentiation matrices.

In this paper, we have modeled the propagation of ultrasonic guided waves in a composite plate by the spectral method. The aim of this work is to have all the information about the modes present in the composite plate as well as its vibratory states. To do this, the mathematical formulation of the problem is explained. After that, we applied the algorithm of the spectral method for plotting the dispersion curves. These curves are plotted for different fiber orientations in order to prove the robustness of the method against different mechanical behaviors. The results obtained are compared with those of the DISPERSE software presented by PAVLAKOVIC *et al.* [17] and considered leading in the field of UGW modeling and analysis based on the GMM. A discussion concerning the computation time and the convergence of the method is set up.

To facilitate the characterization of the different modes obtained in the dispersion curves, we have developed a technique based on the property of displacement symmetry. This technique was able to separate and characterize the different modes that can propagate in the composite plate.

Moreover, the displacements from the spectral method are normalized in amplitudes, so they vary between minus one and one. These have no physical

meaning. To overcome this challenge, we propose to normalize the displacement profiles by the acoustic power. The results obtained are compared with those calculated analytically. A perfect agreement was noticed in both cases of comparison (displacement and stresses). With the proposed normalization, we could show the accuracy of the eigenvectors from the spectral method and give them a physical meaning. Finally, a study of the internal displacements and stresses was established to identify the modes capable of propagating at a determined frequency. All this information allows to establish an adequate procedure for ultrasonic non-destructive testing by UGW of the graphite-epoxy composite plate.

2. FORMULATION OF THE SPECTRAL METHOD

We consider a homogeneous orthotropic waveguide unlimited in the x_1 and x_2 directions, of thickness $e = 2h$ following the direction x_3 (normal to the plate) (Fig. 1).

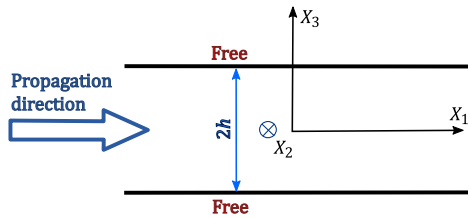


FIG. 1. Waveguide geometry.

The calculations are performed in the global reference system (reference system associated with the crystal) in which the UGW propagates along the x_1 direction with the independence of the properties according to the x_2 coordinate ($\partial/\partial x_2 = 0$). Note that in the general case, the global and reference systems are related by a rotation angle ϕ (Fig. 2). Moreover, the independence of the elastic

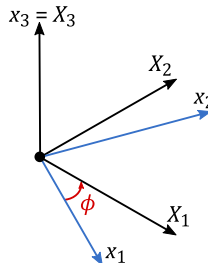


FIG. 2. Global Cartesian coordinate system (x_1, x_2, x_3) and Cartesian reference system (X_1, X_2, X_3) .

behavior of the plate keeps Hooke's law, the deformation-displacement relation and the equations of motion unchanged as long as the elements of the stiffness tensor are transformed by the following relation:

$$(2.1) \quad C_{mnop} = \alpha_{mi}\alpha_{nj}\alpha_{ok}\beta\alpha_{pl}C'_{ijkl} \quad (i, j, k, l, m, n, o, p = 1, 2, 3),$$

where α_{mi} , α_{nj} , α_{ok} represents the transformation matrix whose elements are the cosines between the x_i and X_i axes.

Assuming that a harmonic wave propagates in the direction of the fibers $\{x_1\}$, the equations of motion in indicial form for a linear elastic anisotropic homogeneous media are written:

$$(2.2) \quad \frac{\partial \sigma_{ij}}{\partial x_i} = \rho \frac{\partial^2 u_i}{\partial t^2},$$

where ρ is the density of the plate.

Hooke's law and the deformation-displacement relation are defined, respectively:

$$(2.3) \quad \sigma_{ij} = C_{ijkl}\varepsilon_{kl},$$

$$(2.4) \quad \varepsilon_{kl} = \frac{1}{2} \left(\frac{\partial u_k}{\partial x_l} + \frac{\partial u_l}{\partial x_k} \right).$$

The components of the displacement field that satisfy Eq. (2.2) are written as:

$$(2.5) \quad u_j = U_j(x_3)e^{i(kx_1 - \omega t)}, \quad j = 1, 2, 3,$$

where k is the wave number and ω is the angular pulsation.

By replacing Eq. (2.5) in Eq. (2.2), we find the form of a problem with eigenvalues and eigenvectors written in the following form:

$$(2.6) \quad [A_{nm}] \{U_n\} = -\rho\omega^2 [I] \{U_n\},$$

where $[A_{nm}]$ is a square matrix of $3N$ lines and $3N$ columns, $\{U_n\}$ is a column vector of $3N$ lines, and $[I]$ is the unit matrix of $3N$ lines and $3N$ columns.

The expressions of the different components of the matrix $[A_{nm}]$ are given in (2.7):

$$\begin{aligned}
 (2.7) \quad A_{11} &= -k^2 C_{11} + C_{55} \frac{\partial^2}{\partial x_3^2}, & A_{12} &= 0, \\
 A_{13} &= ik(C_{13} + C_{55}) \frac{\partial}{\partial x_3}, & A_{21} &= 0, \\
 A_{22} &= -k^2 C_{66} + C_{44} \frac{\partial^2}{\partial x_3^2}, & A_{23} &= 0, \\
 A_{31} &= ik(C_{13} + C_{55}) \frac{\partial}{\partial x_3}, & A_{32} &= 0, \\
 A_{33} &= -k^2 C_{55} + C_{33} \frac{\partial^2}{\partial x_3^2}.
 \end{aligned}$$

In the same way, the boundary conditions are written in the following form:

$$(2.8) \quad [BC_{nm}]_{(3N,3N)} \{U_n(\pm h)\}_{(3N,1)} = \{0\}_{(3N,1)}.$$

With the constituents of the matrix $[BC_{nm}]$:

$$\begin{aligned}
 (2.9) \quad BC_{11} &= ikC_{13}, & BC_{13} &= C_{33} \frac{\partial}{\partial x_3}, \\
 BC_{21} &= 0, & BC_{22} &= C_{44} \frac{\partial}{\partial x_3}, \\
 BC_{23} &= 0, & BC_{31} &= C_{55} \frac{\partial}{\partial x_3}, \\
 BC_{32} &= 0, & BC_{33} &= ikC_{55}.
 \end{aligned}$$

The expressions of the elastic constants C_{ij} are given as a function of the engineering constants in (2.10):

$$\begin{aligned}
 (2.10) \quad C_{11} &= \frac{1 - \nu_{23}\nu_{32}}{D} E_1, & C_{12} &= \frac{\nu_{13}\nu_{32} + \nu_{12}}{D} E_2, \\
 C_{13} &= \frac{\nu_{12}\nu_{23} + \nu_{13}}{D} E_3, & C_{22} &= \frac{1 - \nu_{13}\nu_{31}}{D} E_2, \\
 C_{23} &= \frac{\nu_{21}\nu_{13} + \nu_{23}}{D} E_3, & C_{33} &= \frac{1 - \nu_{12}\nu_{21}}{D} E_3, \\
 C_{44} &= G_{23}, & C_{55} &= G_{13}, \\
 C_{66} &= G_{12},
 \end{aligned}$$

where E_i represent the Young modulus in the x_i directions, and G_{ij} and ν_{ij} are the shear modulus and the Poisson coefficients in the (ox_ix_j) planes with $i, j = 1, 2, 3$, respectively.

The system is defined, the spectral method generates nonuniform N collocation points along the thickness, the coordinates of these points are known, and the application of the Chebyshev approximation is implemented to approximate the partial derivatives in x_3 by differentiation matrices noted $D^n = [DM_{cheb}]_{N,N}^n$. And then we rearrange these matrices in the domain of study $[-h, h]$ as follows:

$$(2.11) \quad \Delta^n = (h^{-1})^n D^n.$$

The partial derivatives in x_3 that govern our problem are first-order $\left(\frac{\partial}{\partial x_3}\right)$ and second-order $\left(\frac{\partial^2}{\partial x_3^2}\right)$ partial derivatives. These partial derivatives are going to be generated by the Chebyshev approximation as first and second-order differentiation matrices $\left(D_{(N,N)}^1, D_{(N,N)}^2\right)$. WEIDEMAN and REDDY [18] developed a MATLAB function `chebdif` that computes the differentiation matrices in Chebyshev nodes.

The resolution of the eigenvalue and eigenvector problems in MATLAB is conducted using the `eig` function which provides a diagonal matrix of generalized eigenvalues and another complete matrix whose columns are the corresponding eigenvectors.

Several modes are susceptible to propagating in the plate during the generation of guided waves, and they differ according to the type of symmetry that the material presents. For example, in anisotropic plates (orthotropic, transverse isotropic and cubic at an angle $\phi = 0^\circ$), we find the coexistence of the symmetrical (S_n) and the anti-symmetrical (A_n) Lamb modes as well as symmetrical (SHS_n) and anti-symmetrical (SHA_n) horizontal shear modes, and Lamb modes are uncoupled from horizontal shear modes.

Generally, when the Lamb modes are coupled to SH modes, the phenomenon of mode crossing is always observed in the dispersion curves. To solve this problem, we exploit the symmetry and anti-symmetry properties of the Lamb and SH modes to classify the results obtained. The Lamb pure modes are characterized by the displacement component u_2 which is zero on both sides of the plate thickness ($u_2(+h) = u_2(-h) = 0$), symmetric modes have the longitudinal components of displacement u_1 that are equal on either side of the plate thickness ($u_1(+h) \cdot u_1(-h) > 0$), while the transverse components u_3 are opposite ($u_3(+h) \cdot u_3(-h) < 0$). For anti-symmetric modes, it is the opposite.

The horizontal shear modes are polarized in the x_2 direction, so they are characterized by the components u_1 and u_3 being nonexistent across the thickness of the plate. Similarly, we find the two types of waves SHS_n and SHA_n

whose displacement components u_2 across the plate thickness are respectively equal and opposite ($u_2(+h) \cdot u_2(-h) > 0$) ($u_2(+h) \cdot u_2(-h) < 0$).

For materials with monoclinic symmetry, the Lamb modes are coupled to the SH modes giving place to the generalized Lamb modes. In the same way, they can be divided into symmetric and anti-symmetric modes. The symmetric modes have equal displacement components u_1 and u_2 on both sides of the plate ($u_1(+h) \cdot u_1(-h) > 0$, $u_2(+h) \cdot u_2(-h) > 0$), and opposite for the u_3 components ($u_3(+h)u_3(-h) < 0$). An inverse behavior is taken for anti-symmetric waves.

In the literature, several authors used spectral methods to plot dispersion curves for different types of materials and geometries [14–16], but in all these works, there was no technique to separate these guided modes.

3. DISPLACEMENT AND STRESS FIELDS NORMALIZED BY ACOUSTIC POWER

We now look to normalize the displacement field obtained from the eig function by the acoustic power to be able to perform an energy analysis and after that detect defects and provide a physical meaning to the displacement and stress fields.

The expression of the acoustic power [20] exerted by a mode along the $\{x_1\}$ direction through a section located in the (Ox_2x_3) plane with a length of 1 m in the $\{x_2\}$ direction and a thickness of h along the $\{x_3\}$ axis is written:

$$(3.1) \quad P = -\frac{1}{2} \operatorname{Re} \left(\int_{-h}^{+h} (v^* \cdot \sigma) \mathbf{n} dx_2 \right),$$

where v^* is the conjugate of the velocity vector and σ is the stress tensor.

In addition to the eigenvalues obtained by the eig function of MATLAB, which represents the dispersion curves, we also have the eigenvectors, which represent the eigenvectors. In order to calculate the spectral stresses, we similarly adopt the differentiation matrix to approximate the partial derivatives and subsequently obtain numerical stresses. Also, these stresses are normalized in amplitude. In the same way as for the displacements, we normalize them in acoustic power.

The expression for the normalized displacements and stresses are given in Eqs. (3.2) and (3.3), respectively:

$$(3.2) \quad u_{1N} = \frac{u_1}{\sqrt{|P|}}, \quad u_{2N} = \frac{u_2}{\sqrt{|P|}}, \quad u_{3N} = \frac{u_3}{\sqrt{|P|}},$$

$$(3.3) \quad \sigma_{33N} = \frac{\sigma_{33}}{\sqrt{|P|}}, \quad \sigma_{23N} = \frac{\sigma_{23}}{\sqrt{|P|}}, \quad \sigma_{13N} = \frac{\sigma_{13}}{\sqrt{|P|}},$$

4. DISPERSION CURVES OF THE GRAPHITE-EPOXY COMPOSITE PLATE

In order to validate our results, we used the DISPERSE software [17] based on the GMM, which can handle a multitude of material types. This software has been approved by many authors [12, 21].

For our application, we considered a graphite-epoxy composite plate of 4 mm thickness. This material has the same behavior as a transversely isotropic material for angles $\phi = 0$ and 90° , and similar behavior to a monoclinic material when $\phi = 60^\circ$. The mechanical properties of this composite are reported in Table 1. The values of these engineering constants were taken from Nayfeh's book [19].

Table 1. Engineering constants [19] of a graphite-epoxy composite plate ($\rho = 1.6 \text{ g/cm}^3$).

E_1 [GPa]	E_2 [GPa]	E_3 [GPa]	G_{12} [GPa]	G_{13} [GPa]	G_{23} [GPa]	ν_{12}	ν_{13}	ν_{23}
154.25	14.7276	14.7276	7.46	7.46	5.81	0.182446	0.182446	0.267432

Figure 3 shows the dispersion curves in the (fe, V_P) plane for the three values of the ϕ angle. The dispersion curves obtained by the spectral method are superposed on those from the DISPERSE software. A very good agreement between the two results is noticed. Using the mode separation method

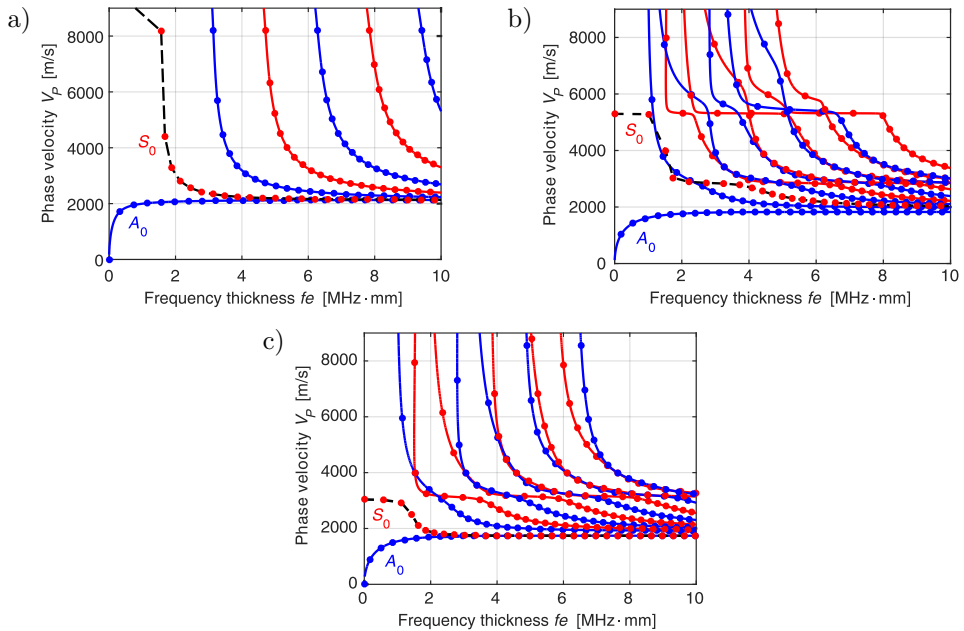


FIG. 3. Dispersion curves in the (feV_P) plane plotted by the spectral method (dotted lines) and the DISPERSE software (continuous lines) for angles of $\phi = 0^\circ$, 60° , and 90° , respectively (a), (b) and (c).

explained in the previous section, we have succeeded in differentiating symmetric Lamb modes from anti-symmetric modes and symmetric SH modes from anti-symmetric modes (Fig. 4). The DISPERSE software has some problems with plotting some modes, such as the S_0 mode (shown in black dotted line (Fig. 3)), despite the fact that it is the most used mode in the UGW control [22, 23]. The spectral method is able to find all the wave modes susceptible to propagate in the composite plate and with a very short computation time of about 0.29 s for a number of collocation points $N = 10$, which is not the case of the root finding algorithm methods and the DISPERSE software. This shows the great advantage of using the spectral method to plot the dispersion curves and having a benefit of computational time with a 10^{-5} order of accuracy compared to the analytical results.

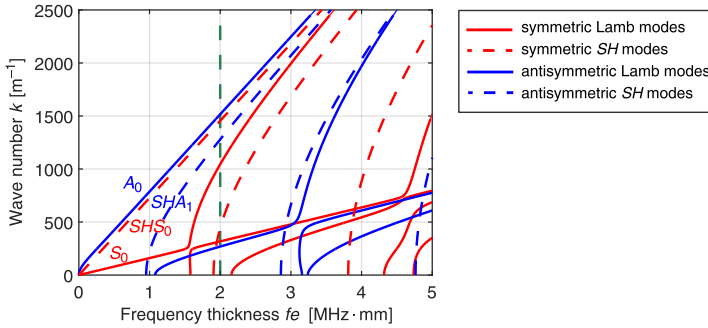


FIG. 4. Dispersion curves in the (fe, k) plane.

5. DISPLACEMENT AND STRESS PROFILES ALONG THE COMPOSITE THICKNESS

In this section, we present the post-treatments of the results from the spectral method compared to the results calculated analytically.

At the frequency $f = 500$ kHz (in Fig. 4 marked by the vertical line in green), we find the following modes respectively: A_1 , S_1 , SHS_1 , S_0 , SHA_1 , SHS_0 and A_0 whose wavenumbers are respectively 271, 316, 441, 1100, 1281, 1456, and 1500 rad/m.

The displacement and stress fields vary according to the amplitudes which makes the application of an energy balance impossible, and consequently we cannot obtain valid information about the defects. To remedy this, we normalize the displacement and stress fields by the acoustic power (Eqs. (3.2) and (3.3)), which will ensure their invariance.

Figure 5 shows the profiles of displacements and stresses according to symmetric and anti-symmetric modes that propagate at a frequency of 500 kHz in

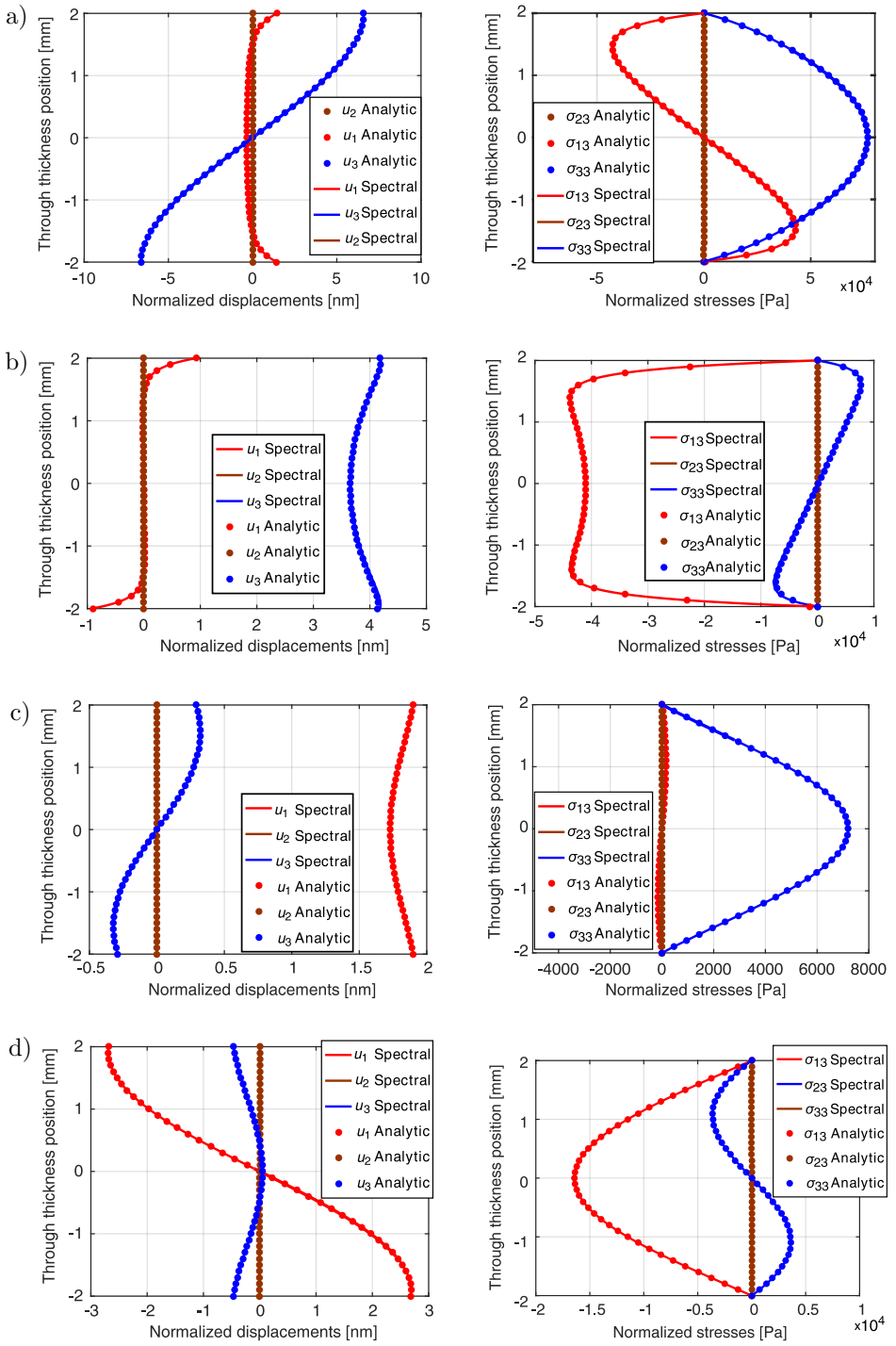


[FIG. 5].

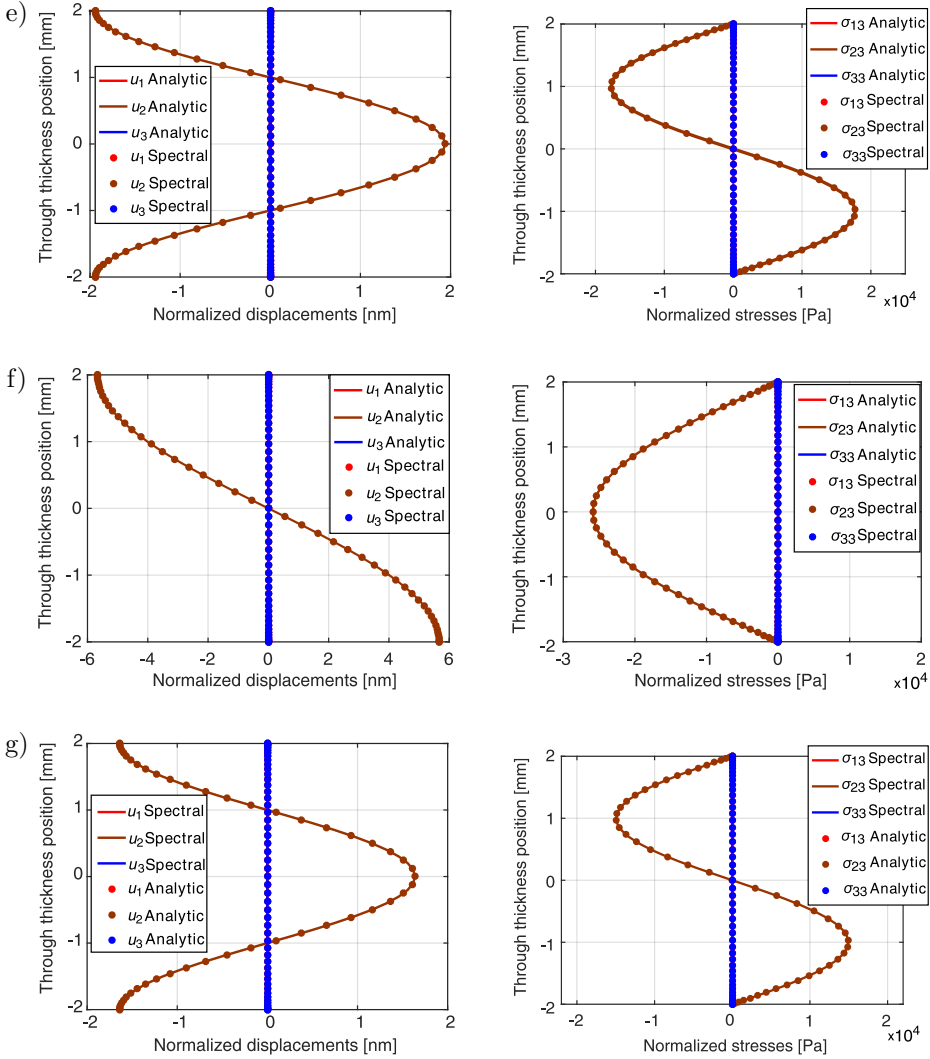


FIG. 5. Normalized displacements and corresponding stresses of the S_0 (a), A_0 (b), S_1 (c), A_1 (d), SHS_0 (e), SHA_1 (f), and SHS_1 (g) modes located at a frequency of $f = 500$ kHz.

the composite. The superposition of the analytical and spectral profiles of displacements and stresses shows an approximate error of 10^{-4} . This error shows the performance of the spectral method in generating the displacement and stress profiles of the modes susceptible to propagating in the composite plate.

The symmetric modes S_0 , S_1 and anti-symmetric modes A_0 , A_1 are Lamb modes characterized by the nullity of the u_2 displacement.

The symmetric modes have the longitudinal and transverse movements along the plate thickness symmetric and anti-symmetric, respectively (Figs. 5a, 5c).

The stress profiles of these modes show us that the symmetric aspect is observed in σ_{33} and the anti-symmetric aspect for σ_{13} .

The anti-symmetric modes A_0, A_1 (Figs. 5b, 5d) have opposite behavior, the displacement u_1 is anti-symmetric while the displacement u_3 is symmetric along the thickness of the composite. The normal stress σ_{33} is then anti-symmetric, and the stress σ_{13} is symmetric.

Horizontal shear modes are modes polarized along the x_2 direction, so they are characterized by the nullity of the u_1 and u_3 components and the non-nullity of the u_2 component (Figs. 5e, 5f, and 5g), which leads to the nullity of the stresses σ_{33} and σ_{13} and the non-nullity of the stress σ_{23} . The u_2 component and the σ_{23} stress can be either symmetric or non-symmetric along the plate thickness, depending on the nature of the mode.

Furthermore, we can see that the stresses σ_{33}, σ_{23} , and σ_{13} at $x_3 = \pm h$ are zero, which shows that the free plate boundary conditions are confirmed.

Finally, the dispersion curves allow us the knowledge of the adequate frequencies for non-destructive testing by UGW. The vibratory analysis of displacements and stresses gives us information on the nature of the modes that can be generated at a specific frequency.

During the ultrasonic inspection of a piece, the sensors are placed in direct contact or close to one of the two surfaces of the piece. Generally, these sensors measure normal displacements at the plate surface and convert them into electrical signals for visualization and interpretation. The knowledge of the amplitudes of the normal displacements at the surface of the plate is essential since they determine the wave that will be more easily generated and/or detected during the inspection and also allow the calculation of the reflection and transmission coefficients when the wave interacts with a defect. In Fig. 6, we have represented the evolution of the normal displacements collected at the upper surface of the plate as a function of the thickness frequency product. At low

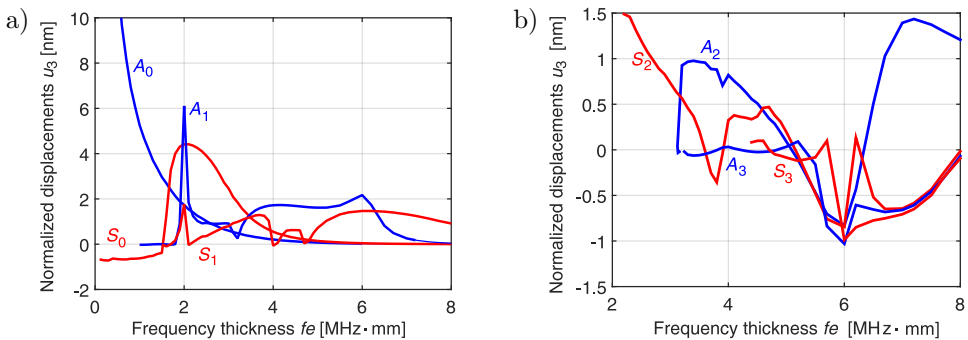


FIG. 6. Normalized displacement u_3 as a function of the frequency thickness product taken at the top surface ($x_3 = h$) of a graphite-epoxy composite plate ($\phi = 0^\circ$) of the $S_0, A_0, S_1,$ and A_1 (a), $S_2, A_2, S_3,$ and A_3 (b) modes.

frequencies, the fundamental mode A_0 has higher amplitudes of normal displacement. These latter decrease with the increase in frequency. While the symmetric fundamental mode S_0 , for $fe \leq 1.5 \text{ MHz} \cdot \text{mm}$, shows a negative displacement. Beyond this value, the displacement increases until reaching a maximum value at $fe \approx 2 \text{ MHz} \cdot \text{mm}$. After that, it decreases to converge to the same order as the A_0 mode displacements. For the higher-order modes, the displacements appear only from certain values called cutoff frequencies. For example, the cutoff frequency of the A_1 mode is 250 kHz and 375 kHz for the S_1 mode. This cutoff frequency increases with the order of the mode. At high frequencies, these modes maintain a considerable vibratory state on the surface compared to the fundamental modes. This information is very important when it comes to choosing the most appropriate mode to generate and provide crucial information on the health of the piece inspected.

6. CONCLUSION

The spectral method offers a very efficient way to plot the dispersion curves of a graphite-epoxy composite material according to different behaviors (transversely isotropic for angles of and 90° as well as monoclinic behavior for an angle of 60°). It is simple to implement, fast, and has an exponential convergence. The accuracy of the solutions was demonstrated when we compared them with those obtained by the DISPERSE software. The technique of separation of the modes susceptible to propagate in the plate that we have developed has allowed us to distinguish between the different types of modes and their symmetry character and for different mechanical behavior (transverse isotropic and monoclinic).

Moreover, with the help of the normalization of the spectral displacement profiles by the acoustic power, we could provide an adequate physical meaning to the eigenvectors. A comparison was made with the analytical displacements and stresses, which showed a very good agreement and reflected the accuracy of the approach developed. The knowledge of the modes able to propagate in the composite at a given frequency allows the implementation of a numerical and experimental procedure of non-destructive ultrasonic testing by UGW of the studied composite, which will allow us to achieve a better characterization of the defects. As a perspective for future work, we will test the spectral method for complex structures (cylindrical and multilayered) as well as to analyze the non-propagating and attenuated modes of viscoelastic structures.

DECLARATION

Conflict of Interest: On behalf of all the authors, the corresponding author declares that there is no conflict of interest in the publication of this paper.

REFERENCES

1. LEE D.G., SUH N.P., *Axiomatic Design and Fabrication of Composite Structures: Applications in Robots, Machine Tools, and Automobiles*, Oxford University Press, New York 2005.
2. LUKEZ R., The use of graphite/epoxy composite structures in space applications, *1st Annual USU Conference on Small Satellites*, 1987.
3. HARB M.S., YUAN F.G., Non-contact ultrasonic technique for Lamb wave characterization in composite plates, *Ultrasonics*, **64**: 162–169, 2016, doi: 10.1016/j.ultras.2015.08.011.
4. KATZ T., MACKIEWICZ S., RANACHOWSKI Z., KOWALEWSKI Z.L., ANTOLIK Ł., Ultrasonic detection of transversal cracks in rail heads—theoretical approach, *Engineering Transactions*, **69**(4): 437–456, 2021, doi: 10.24423/EngTrans.1695.20211220.
5. MATSUO T., HATANAKA D., Development of non-contact fatigue crack propagation monitoring method using air-coupled acoustic emission system, *Engineering Transactions*, **67**(2): 185–198, 2019, doi: 10.24423/EngTrans.1009.20190405.
6. GUO S., REBILLAT M., MECHBAL N., Dichotomy property of dispersion equation of guided waves propagating in anisotropic composite plates, *Mechanical Systems and Signal Processing*, **164**: 108212, 2022, doi: 10.1016/j.ymssp.2021.108212.
7. NDIAYE E.B., DUFLO H., Non destructive testing of sandwich composites: adhesion defects evaluation; experimental and finite element method simulation comparison, [in:] *Proceedings of the Acoustics 2012 Nantes Conference*, April 23–27, 2012, Nantes, France, pp. 2659–2664.
8. ROKHLIN S.T., CHIMENTI D.E., NAGY P.B., *Physical Ultrasonics of Composites*, Oxford Academic Press, 2011, doi: 10.1093/oso/9780195079609.001.0001.
9. YU J.G., ZHANG B., LEFEBVRE J.E., ZHANG C.H., Wave propagation in functionally graded piezoelectric rods with rectangular cross-section, *Archives of Mechanics*, **67**(3): 213–231, 2015.
10. ZHANG X.M., YU J.G., Effects of initial stresses on guided waves in unidirectional plates, *Archives of Mechanics*, **65**(1): 3–26, 2013.
11. ZHANG X., LIANG S., SHAO S., YU J., A quadrature-free Legendre polynomial approach for the fast modelling guided circumferential wave in anisotropic fractional order viscoelastic hollow cylinders, *Archives of Mechanics*, **73**(2): 121–152, 2021, doi: 10.24423/aom.3642.
12. BARAZANCHY D., GIURGIUTIU V., A comparative convergence and accuracy study of composite guided-ultrasonic wave solution methods: Comparing the unified analytic method, SAFE method and DISPERSE, *Proceedings of the Institution of Mechanical Engineers, Part C: Journal of Mechanical Engineering Science*, **231**(16): 2961–2973, 2017, doi: 10.1177/0954406217700928.
13. HEBAZ S.E., BENMEDDOUR F., MOULIN E., ASSAAD J., Semi-analytical discontinuous Galerkin finite element method for the calculation of dispersion properties of guided waves in plates, *The Journal of the Acoustical Society of America*, **143**(1): 460–469, 2018, doi: 10.1121/1.5021588.
14. ADAMO A.T.I., CRASTER R.V., Spectral methods for modelling guided waves in elastic media, *The Journal of the Acoustical Society of America*, **116**(3): 1524–1535, 2004, doi: 10.1121/1.1777871.

15. KARPFFINGER F., GUREVICH B., BAKULIN A., Modeling of wave dispersion along cylindrical structures using the spectral method, *The Journal of the Acoustical Society of America*, **124**(2): 859–865, 2008, doi: 10.1121/1.2940577.
16. QUINTANILLA F.H., LOWE M.J.S., CRASTER R.V., Modeling guided elastic waves in generally anisotropic media using a spectral collocation method, *The Journal of the Acoustical Society of America*, **137**(3): 1180–1194, 2015, doi: 10.1121/1.4913777.
17. PAVLAKOVIC B., LOWE M., ALLEYNE D., CAWLEY P., Disperse: A general purpose program for creating dispersion curves, [in:] Thompson D.O., Chimenti D.E. [Eds] *Review of Progress in Quantitative Nondestructive Evaluation*, vol. 16, pp. 185–192, Springer, Boston, MA, 1997, doi: 10.1007/978-1-4615-5947-4_24.
18. WEIDEMAN J.A., REDDY S.C., A MATLAB differentiation matrix suite, *ACM Transactions on Mathematical Software (TOMS)*, **26**(4): 465–519, 2000, doi: 10.1145/365723.365727.
19. NAYFEH A.H., *Wave Propagation in Layered Anisotropic Media: with Application to Composites*, Elsevier, 1995.
20. RHIMINI H., EL ALLAMI M., SIDKI M., HADDOUT A., BENHADOU M., Ultrasonic guided waves in tri-layer structure. Application to study the interaction of guided waves with hidden defect at low frequency, *Technical Acoustics (Техническая акустика)*, **16**: 1–14, 2016.
21. HERNANDEZ-CRESPO B., ENGINEER B., COURTNEY C., Empirical technique for dispersion curve creation for guided wave applications, [in:] *8th European Workshop on Structural Health Monitoring*, July 5–8, 2016 in Bilbao, Spain, pp. 1375–1384, *e-Journal of Nondestructive Testing*, **21**(8), <https://www.ndt.net/?id=19911>.
22. MORI N., BIWA S., Transmission characteristics of the S0 and A0 Lamb waves at contacting edges of plates, *Ultrasonics*, **81**: 93–99, 2017, doi: 10.1016/j.ultras.2017.06.009.
23. BENMEDDOUR F., GRONDEL S., ASSAAD J., MOULIN E., Experimental study of the A0 and S0 Lamb waves interaction with symmetrical notches, *Ultrasonics*, **49**(2): 202–205, 2009, doi: 10.1016/j.ultras.2008.08.002.

Received November 22, 2022; accepted version March 3, 2023.



Copyright © 2023 The Author(s).

This is an open-access article distributed under the terms of the Creative Commons Attribution-ShareAlike 4.0 International (CC BY-SA 4.0 <https://creativecommons.org/licenses/by-sa/4.0/>) which permits use, distribution, and reproduction in any medium, provided that the article is properly cited. In any case of remix, adapt, or build upon the material, the modified material must be licensed under identical terms.